[14] G. Ghione and C. Naldi, "Coplanar waveguides for MMIC applications: Effects of upper shielding, conductor backing, finite-extent ground planes, and line-to-line coupling," *IEEE Trans. Microwave Theory Tech.*, vol. MTT-35, no. 3, pp. 260–267, 1987.

[15] S. Gevorgian, L. J. P. Linner, and E. L. Kollberg, "CAD models for shielded multilayered CPW," *IEEE Trans. Microwave Theory Tech.*, vol. 43, no. 4, pp. 772–779, 1995.

[16] H. A. Wheeler, "Transmission-line properties of parallel strips separated by a dielectric sheet," *IEEE Trans. Microwave Theory Tech.*, vol. MTT-13, pp. 172–185, 1965.

[17] E. O. Hammerstad, "Equations for microstrip circuit design," in *Proc. 5th European Microwave Conf.*, Hamburg, Germany, 1975, pp. 268–272.

[18] C. P. Wen, "Coplanar waveguide: A surface strip transmission line suitable for nonreciprocal gyromagnetic device applications," *IEEE Trans. Microwave Theory Tech.*, vol. MTT-17, pp. 1087–1090, 1969.

[19] R. K. Hoffmann, *Handbook of Microwave Integrated Circuits*. Norwood, MA: Artech House, 1987.

[20] B. C. Wadell, *Transmission Line Design Handbook*. Norwood, MA: Artech House, 1991.

[21] W. Hilberg, "From approximations to exact relations for characteristics impedances," *IEEE Trans. Microwave Theory Tech.*, vol. MTT-17, no. 5, pp. 259–265, 1969.

[22] P. A. J. Dupuis and C. K. Campbell, "Characteristic impedance of surface-strip coplanar waveguide," *Electron. Lett.*, vol. 9, pp. 354–355, 1973.

[23] K. C. Gupta, R. Garg, and I. J. Bahl, *Microstrip Lines and Slotlines*. Norwood, MA: Artech House, 1979.

[24] M. E. Davis, E. W. Williams, and A. C. Celestini, "Finite-boundary corrections to the coplanar waveguides analysis," *IEEE Trans. Microwave Theory Tech.*, vol. MTT-21, pp. 594–596, 1973.

Lower Order Modes of YBCO/STO/YBCO Circular Disk Resonators

Spartak Gevorgian, Erik Carlsson, Peter Linnér, Erik Kollberg, Orest Vendik, and Erland Wikborg

Abstract—**Lower order modes in a single crystal strontium titanate (STO) circular disk resonator are studied experimentally. Superconducting epitaxial YBCO films form the parallel-plates of the resonator. Due to the extremely high dielectric constant of STO, the electric fields are concentrated between the plates, while there is a substantial magnetic fringing field which affects both the resonant frequencies, Q-factors, and tunability of all modes, especially the TM_{110} and TM_{210}.**

I. Introduction

Electrically controlled-parallel plate resonators based on bulk ferroelectric ceramics have been studied in the past [1]. Single crystal bulk strontium titanate (STO) circular disk resonators with thin, epitaxial $YBa_2Cu_3O_{7-x}$ (YBCO) plates have recently demonstrated superior performance both in the sense of higher Q-factors and controllability at frequencies between 1 and 2 GHz when cooled to liquid nitrogen (LN) temperature (77 K) [2]. These devices show a great potential for a wide range of applications in Cellular Communication and other microwave systems in the frequency range 0.5–3.0 GHz due to their low microwave losses, the electric field/temperature controllability of the STO dielectric constant around LN temperatures, and the integration of high temperature superconductors (HTS, e.g., YBCO). A drastic size reduction for microwave components in this frequency range can be achieved due to the extremely high dielectric constant of STO. Although the results reported in [2] are encouraging, an extra study of modal performance of YBCO/STO/YBCO parallel-plate resonators is needed to meet the requirements of Cellular Communication Systems and other low frequency microwave systems where size reduction and electrical tunability are critical issues. In this work we report on the results of an experimental study of the lower order modes in a YBCO/STO/YBCO parallel-plate circular disk resonator. In contrast with the work reported in [2] two lower order modes have been excited with lower resonant frequencies for the same resonator diameter offering additional size reduction and more potential in system level applications. The electric field is highly concentrated between the plates of the resonator due to the large dielectric constant while there is a substantial magnetic stray field, especially for lower order modes. This magnetic stray field strongly affects both the resonance frequency, Q-factor, and tunability of the YBCO/STO/YBCO resonator.

Manuscript received September 29, 1995; revised June 14, 1996. This work was supported in part by the NORdic Program on Applied Superconductivity (NORPAS) and by the Swedish material consortium on high-T_c superconductivity

S. Gevorgian, E. Carlsson, P. Linnér, and E. Kollberg are with the Department of Microwave Technology, Chalmers University of Technology, S-412 96 Göteborg, Sweden.

O. Vendik is with the Department of Electronics, Electrotechnical University, St. Petersburg, Russia.

E. Wikborg is with the Fiber Optics Research Center, Ericsson Components AB, S-164 81 Stockholm, Sweden.

Publisher Item Identifier S 0018-9480(96)06912-8.

TABLE I
Modal Parameters of Disk Resonator

Mode number	Modes, TM_{nm0}	k_{nm}
1	TM_{010}	0
2	TM_{110}	1.8412
3	TM_{210}	3.0542
4	TM_{020}	3.8317
5	TM_{310}	4.2012
6	TM_{410}	5.3176
7	TM_{120}	5.3314
8	TM_{510}	6.4156
9	TM_{220}	6.7061

II. Simple Theoretical Background

A. TM Modes of a Thin Parallel-Plate Circular Disk Resonator

The resonator geometry is shown in Fig. 1. Assuming a magnetic wall at the edges of the disk [1]–[3] the following equation for the resonant frequency is obtained:

$$f_{nm} = \frac{c_o k_{nm}}{2\pi r_o \sqrt{\varepsilon_r}} \quad (1)$$

with c_o being the free space light velocity, r_o the radius of the disk, and ε_r the relative dielectric constant of the dielectric (e.g. STO). k_{nm} is the mth zero of the derivative of the Bessel function

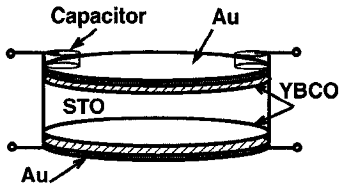

Fig. 1. The geometry of the YBCO/STO/YBCO resonator with coupling capacitances.

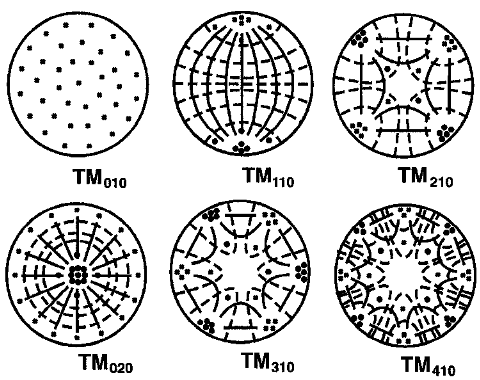

Fig. 2. Mode chart of the six lowest order TM modes in a circular disk resonator. Solid lines are current, dashed lines are the magnetic field, dots and crosses are the electric field.

of order n. Table I summarizes some lower order TM_{nmp} modes of a circular parallel-plate resonator. The mode indices are given according to the Bessel function order/root [4]. Note that $p = 0$ is assumed for all modes, i.e., it is supposed that the thickness of the disk is smaller than half a wavelength and the resonator supports only TM_{nm0} modes. The roots in Table I are given in increasing order starting with TM_{010}. For this mode $k_{01} = 0$, which indicates an infinite wavelength. This is the electrostatic case where the plates of the resonator are charged uniformly. Following [3] Fig. 2 displays the field/current distributions of the six lowest order modes of the resonator. In Fig. 2 and Table I mode indices correspond to n and m in k_{nm}, hence the mode reported in [1] and [2] is TM_{020} in this notation.

B. The Dielectric Constant of STO

Precise knowledge of the dielectric constant of STO is a critical issue in modeling the resonance frequency of these resonators. The dielectric constant of bulk single crystal STO is known to be independent of frequency up to 100–200 GHz [5], [6]. For accurate modeling of the dielectric constant we made 1 kHz capacitive bridge measurements of the dielectric constant for the STO crystals. The temperature dependence of the STO dielectric constant for dc electric fields of 0, 5, and 10 kV/cm are shown in Fig. 3(a) while the bias dependence of the dielectric constant at different temperatures is given in Fig. 3(b). The experimental temperature and field dependencies of the dielectric constant of bulk STO, in Fig. 3, may be accurately modeled using the analytical relations for the STO dielectric constant given in [5].

III. Microwave Characterization of the Resonator

In the microwave measurements we used STO circular disks, diameter $2r_o = 10$ mm and thickness $h = 0.5$ mm, similar to the one reported in [2]. Double-sided 0.2 μm thick YBCO films were deposit by E. Hollman and A. Zaitsev, Electrical Engineering University, St. Petersburg, Russia. The surface resistance of the films

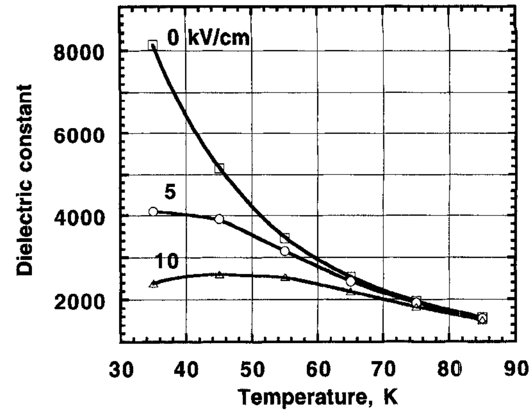

(a)

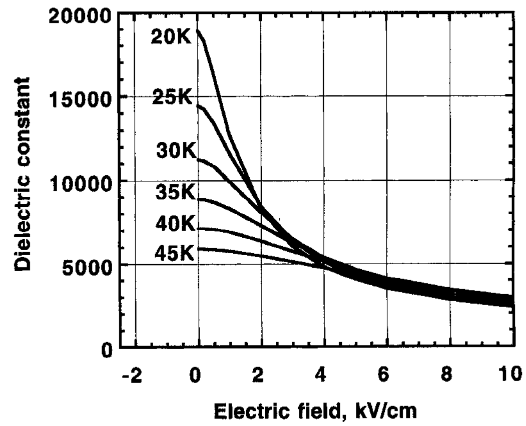

(b)

Fig. 3. (a) Temperature dependence of the STO dielectric constant at different dc electric fields. (b) Electric field dependence of the STO dielectric constant.

at 77 K, 60 GHz was measured to be 20–40 mΩ with $T_c = 89$–91 K. Using a ω^2 frequency dependence for the surface resistance this corresponds to 0.55–1.1 mΩ at 10 GHz and 77 K. Afterwards the films were coated with a 0.4 μm thick gold layer using vacuum evaporation. The films have been cooled several times to measure the STO dielectric constant. Resonator measurements were performed 4–5 months after film preparation. To excite $\mathrm{TM}_{110}, \mathrm{TM}_{210}$ and other modes the resonator was mounted into a test fixture with K-connectors instead of a coaxial fixture as reported in [2]. A simplified measurement set-up is shown in Fig. 1. both capacitive and galvanic couplings have been used. In the case of capacitive coupling, 3.0 pF thin film capacitors have been attached directly to the gold plate, Fig. 1, while in the case of galvanic coupling the pins of the K-connectors were in direct ohmic contact with the gold plate on top of the YBCO film. S-parameters of the resonators were measured using a Wiltron 360B network analyzer. The measured spectrum of resonance frequencies of some lower order modes without external bias at 35 K is shown in Fig. 4. From microwave measurements the estimated T_c is 86–87 K which is 3–4 K less than the T_c of the fresh films.

The coupling into the resonator is very week (of the order of -20 to -40 dB) due to the high dielectric constant of STO and large reflection of microwaves from the edge of the resonator. The temperature and electric field dependence of the loaded Q-factors for several of the lowest order modes are shown in Fig. 5.

The highest Q-factor measured was for the TM_{020} mode, as can be expected from the current distribution, Fig. 2. For a similar resonator

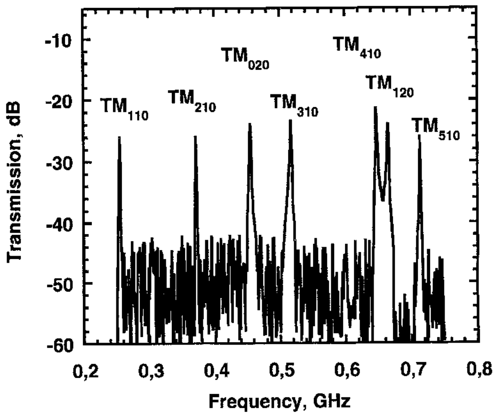

Fig. 4. The measured spectrum of resonant frequencies at 35 K without external electric field bias and with capacitive coupling. The disk diameter was $2r_0 = 10$ mm.

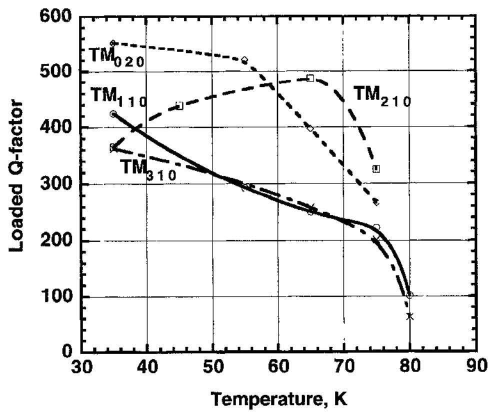

(a)

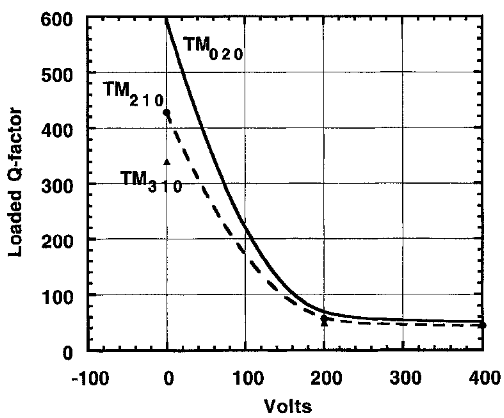

(b)

Fig. 5. (a) Temperature dependence of the Q-factors for several lower order modes ($2r_0 = 10$ mm). (b) The Q-factors for three modes as a function of applied voltage.

in a coaxial test fixture studied in [2] this mode showed much higher Q-factors. Since the measured Q-factors follow a typical HTS temperature dependence, Fig. 5(a), it indicates that the main losses in the resonator are due to the YBCO film and their poor quality. The low Q-factor is due to degradation of the YBCO film. The 0.4 μm thick gold film used for ohmic contacts will also add to the losses. To improve the Q-factor and minimize the influence of the gold layer the YBCO thickness should be larger than the London penetration

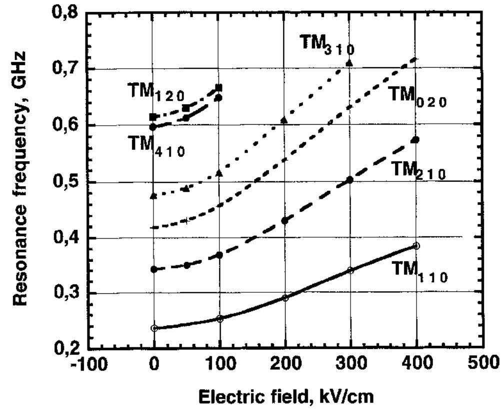

Fig. 6. The measured resonant frequencies for different modes as a function of applied electric field.

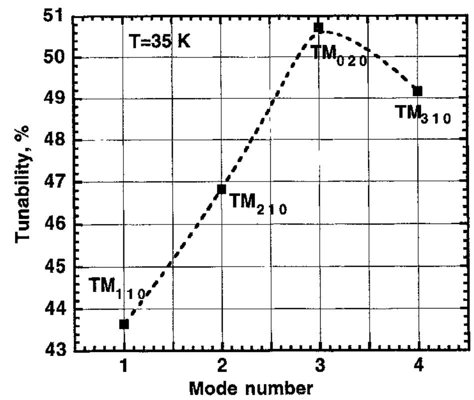

Fig. 7. The measure tunability changing the electric field from 0 to 8 kV/cm at 35 K for the lowest order modes. The dashed line is a guide for the eyes.

depth. Additionally, if the thickness of the gold film is larger than the skin depth one can still expect reasonable high Q-factors in the case of a cooling failure, were the temperature exceeds T_c.

It is worth noting that the Q-factor of the modes decreased with applied voltage, Fig. 5(b). This is in agreement with measurements on bulk single crystal STO [2]. On the other hand from the "soft" transverse phonon model one has to expect a reduction of microwave losses (increase in Q-factor) with increased applied field [5], [6]. Probably along with the "soft" mode there are other competing loss mechanisms. One possible mechanism is piezoelectric transformation of the microwave power. In a bulk STO resonator the piezoelectric effect can be induced by electrostriction which may be enhanced by an acoustic resonance [1]. According to this model the applied field will increase the electrostrictive deformation of the crystal leading to increased piezoelectric transformation of microwave power. The dependence of the resonant frequencies upon applied electric field are shown in Fig. 6. The fractional tunability of the resonantor defined as $T_{nm} = (f_{nm}(400\ \text{V}) - f_{nm}(0\ \text{V}))/f_{nm}(0\ \text{V})$ is larger for higher order modes, as can be seen from Fig. 7. It is largest for the TM_{020} mode which has the highest degree of field confinement.

Modeling the resonant frquency of a circular parallel-plate resonator is rather a historical problem. Early simple magnetic wall models [1], [3] for the resonant frequency (1) of a circular parallel-plate resonator have been improved by using Kirchhoff's capacitance formula and introducing the concept of an effective radius to take into account the static electric stray field (in an air filled disk) [7]. This model has been modified further to include the effect of the dielectric constant [8]–[11]. Due to the extremely large dielectric

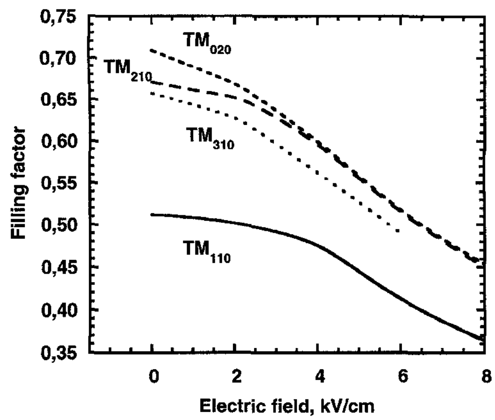

Fig. 8. Filling factor for the lowest order TM modes.

constant of STO the effective radius of the resonator, r_{eff} (estimated using the formula given in [8]), can be replaced by the geometrical radius r_o, with less than 0.03% error. This, in other words, suggests practically no fringing fields. However, using this model extemely poor (15–25%) agreement is observed between measured, Fig. 6, and computed frequencies. Resonant frequencies are computed using (1) and the measured dielectric constant, Fig. 3. The discrepancy may be explained by the fact that the effective radius introduced in [8] suggests no fringing capacitance change when the air filling of the disk is replaced by a dielectric. It suggests only an increase of the main capacitance leading to a relative reduction of the fringing capacitance part of the total capacitance.

In addition to the effective radius the concept of a dynamic dielectric constant, ε_{dyn}, has been introduced [7] to take into account the actual (dynamic) microwave charge (current) distribution in the conducting plates and the dynamic electric stray field. Nevertheless, for all modes the computed ε_{dyn} is substantially larger than what is measured. Hence the theory presented in [7] can not readily be used for modeling the resonant frequency of an STO resonator. The discrepancy between measured and computed dynamic dielectric constants can be explained as follows. For computation of ε_{dyn} in [7] the dynamic capacitance of a circular disk is evaluated first, or in other words, *only* the dynamic electric stray field is taken into account.

In reality there is also a dynamic magnetic stray field which is important in resonant frequency modeling. The dynamic magnetic stray field depends upon the magnetic field distribution of a particular resonant mode. These stray magnetic fields have to be taken into account and treated properly. At this instant the amount of stray field may be estimated using a filling factor defined as [12]

$$q_{nm} = \frac{(\varepsilon\mu)_{nm} - 1}{\varepsilon_r - 1} \tag{2}$$

where ε_r is the relative dielectric constant of STO, Fig. 3, and the $(\varepsilon\mu)$ product is calculated from the measured resonance frequency

$$(\varepsilon\mu)_{nm} = \left(\frac{c_o k_{nm}}{2\pi r_{\text{eff}} f_{nm}}\right)^2 \tag{3}$$

r_{eff} is here the effective radius of the disk taking into account the static stray fields around the disk [7]. It follows from Fig. 8. that despite the extremely high dielectric constant of STO the filling factors of all modes are rather small when compared to a low dielectric constant disk resonator [12]. Moreover, due to the high confinement of magnetic field, Fig. 2, the highest filling factor is found for the TM_{020} mode and the lowest filling factor for the TM_{110} mode, as expected from the field distribution shown in Fig. 2.

IV. Conclusion

Lower order modes in a HTS plated STO parallel-plate circular disk resonator have been studied experimentally. Both tunability and quality factor increase with higher confinement of electromagnetic field. The highest tunability, Q-factors, and electromagnetic field confinement are found for the TM_{020} mode. Large fringing magnetic fields result in a rather small filling factor (despite the large dielectric constant of the STO) which is more pronounced for lower order modes. The effects of fringing magnetic field and surface plasma waves at the HTS/STO interface [13] should be studied carefully to achieve precise modeling of the resonant frequency.

Acknowledgment

The authors would like to thank Prof. J. Helszajn for helpful correspondence.

References

[1] I. G. Mironenko, N. N. Antonov, and V. V. Nezentsev, "Investigation of dielectric losses in $BaTiO_3$ ferroelectric ceramics in the wide frequency band," (in Russian), *Izv. Leningrad Electrotechnical Institute*, 1968, issue 64, pp. 148–156.

[2] O. G. Vendik, E. Kollberg, S. S. Gevorgian, A. B. Kozyrev, and O. I. Soldatenkov, "1 GHz tuneable resonator on bulk single crystal $SrTiO_3$ plated with $YBa_2Cu_3O_{7-x}$ films," *IEEE Electron. Device Lett.*, vol. 37, pp. 654–656, 1995.

[3] J. Watkins, "Circular resonator structures in microstrip," *IEEE Electron. Device Lett.*, vol. 5, pp. 524–525, 1969.

[4] G. N. Watson, *A Treatise on the Theory of Bessel Functions.* Cambridge, MA: University Press, 1962.

[5] O. G. Vendik, "Dielectric nonlinearity of displacive ferroelectrics at UHF," *Ferroelectrics*, 1976, vol. 12, pp. 85–90.

[6] R. C. Neville, B. Honeisen, and C. A. Mead, "Permittivity of Strontium Titanate," *J. Appl. Phys.*, 1972, vol. 43, no. 5, pp. 2124–2131.

[7] I. Wolff and N. Knoppik, "Rectangular and circular microstrip disk capacitors and resonators," *IEEE Trans. Microwave Theory Tech.*, vol. MTT-22, pp. 859–864, 1974.

[8] L. C. Chen, S. A. Long, M. R. Allerding, and M. D. Walton, "Resonant frequency of a circular disc antenna," *IEEE Trans. Antennas Propagat.*, vol. AP-25, pp. 595–596, 1977.

[9] W. C. Chew and J. A. Kong, "Effects of Fringing Fields on the Capacitance of Circular Microstrip Disk," *IEEE Trans. Microwave Theory Tech.*, vol. MTT-28, 2, pp. 98–103, 1980.

[10] T. Itoh and R. Mittra, "A new method for calculating the capacitance of a circular disk for microwave integrated circuits," *IEEE Trans. Microwave Theory Tech.*, pp. 431–432, June 1973.

[11] S. R. Borkar and R. F. H. Yang, "Capacitance of a circular disk for applications in microwave integrated circuits," *IEEE Trans. Microwave Theory Tech.*, pp. 588–591, July 1975.

[12] J. Helszajn, *Microwave Planar Passive Circuits and Filters.* New York: Wiley, 1994.

[13] S. Gevorgian, E. Carlsson, and E. Wikborg, "Fundamental TM mode of a superconducting parallel-plate waveguide," *Inst. Phys. Conf.*, ser. no. 148, pp. 1167–1170, 1995.